

R. Thurman-Keup[#], M. El Baz, V. Scarpine,
Fermi National Accelerator Laboratory, Batavia, USA

Abstract

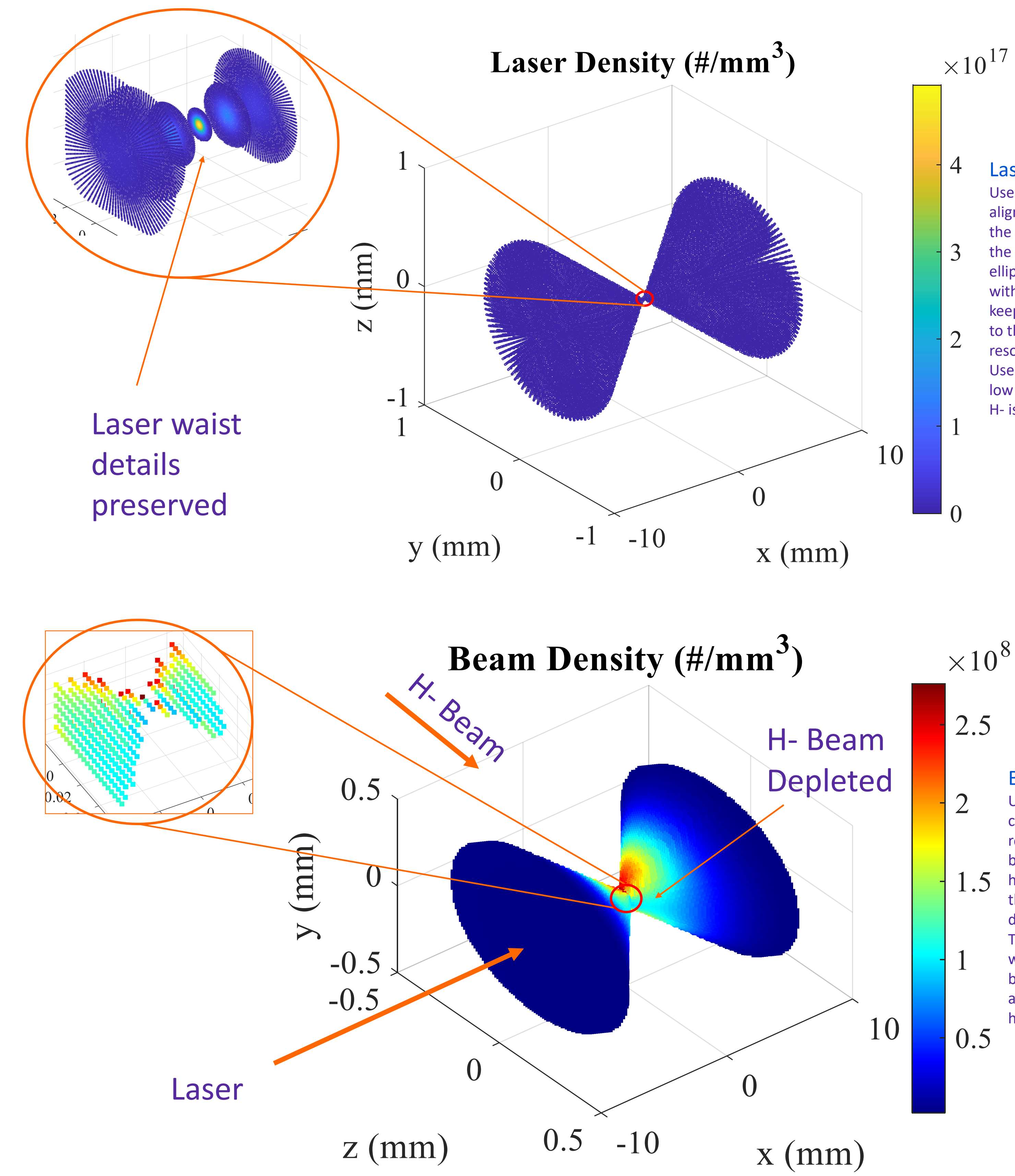
The Proton Improvement Plan - II (PIP-II) is a new linear accelerator (LINAC) complex being built at Fermilab. It is based on superconducting radiofrequency cavities and will accelerate H⁺ ions to 800 MeV kinetic energy before injection into the existing Booster ring. Measurements of the profile of the beam along the LINAC must be done by non-intercepting methods due to the superconducting cavities. The method chosen is photoionization of a small number of H⁻ by a focused infrared laser, aka laserwire. The number of ionized electrons is measured as a function of laser position within the H⁻ beam. To aid in the design of the collection mechanism, a simulation was written in MATLAB with input from the commercial electromagnetic simulation, CST. This simulation calculates the number and positions of the liberated electrons and tracks them through the magnetic collection and H⁻ beam fields to the collection point. Results from this simulation for various points along the LINAC will be shown.

Introduction

Fermilab is in the process of constructing a new super-conducting (SC) linear accelerator to replace the existing normal conducting LINAC. This project is called the Proton Improvement Plan - II (PIP-II) [1] and is being built to increase the deliverable beam intensity to the Deep Underground Neutrino Experiment being constructed in South Dakota. Since the LINAC is mostly superconducting, the use of physical wire scanners as beam profilers is not allowed in much of the LINAC due to the risk of a broken wire contaminating the SC cavities. As the beam is composed of H⁻ ions, laserwires [2,3] were chosen as the profiler. A laserwire functions by photoionization of the extra electron on the H⁻ ion using a focused laser. The binding energy of the extra electron is only 0.7542 eV and can be ionized by a 1064 nm YAG laser. The ionized electrons, which are proportional in number to the local density of H⁻ ions, are collected as the laser is moved through the H⁻ beam, enabling reconstruction of the profile of the beam.

Photoionization Simulation

The simulation code is written in MATLAB [6]. It steps through time and calculates the number of ionized electrons on a predefined set of physical mesh points. The simulation utilizes one of two possible numerical mesh arrangements, laser grid or beam grid, depending on the laser and H⁻ beam parameters.



Photoionization Theory

The number of photoionizations depends on the particle densities of both the incoming laser, I_l , and H⁻ beam, I_b , and the cross section for photoionization, σ_i ,

$$dn = c \sigma_i \int (|\hat{l} - \hat{\beta}|^2 - |\hat{l} \times \hat{\beta}|^2) I_l I_b dt dx dy dz$$

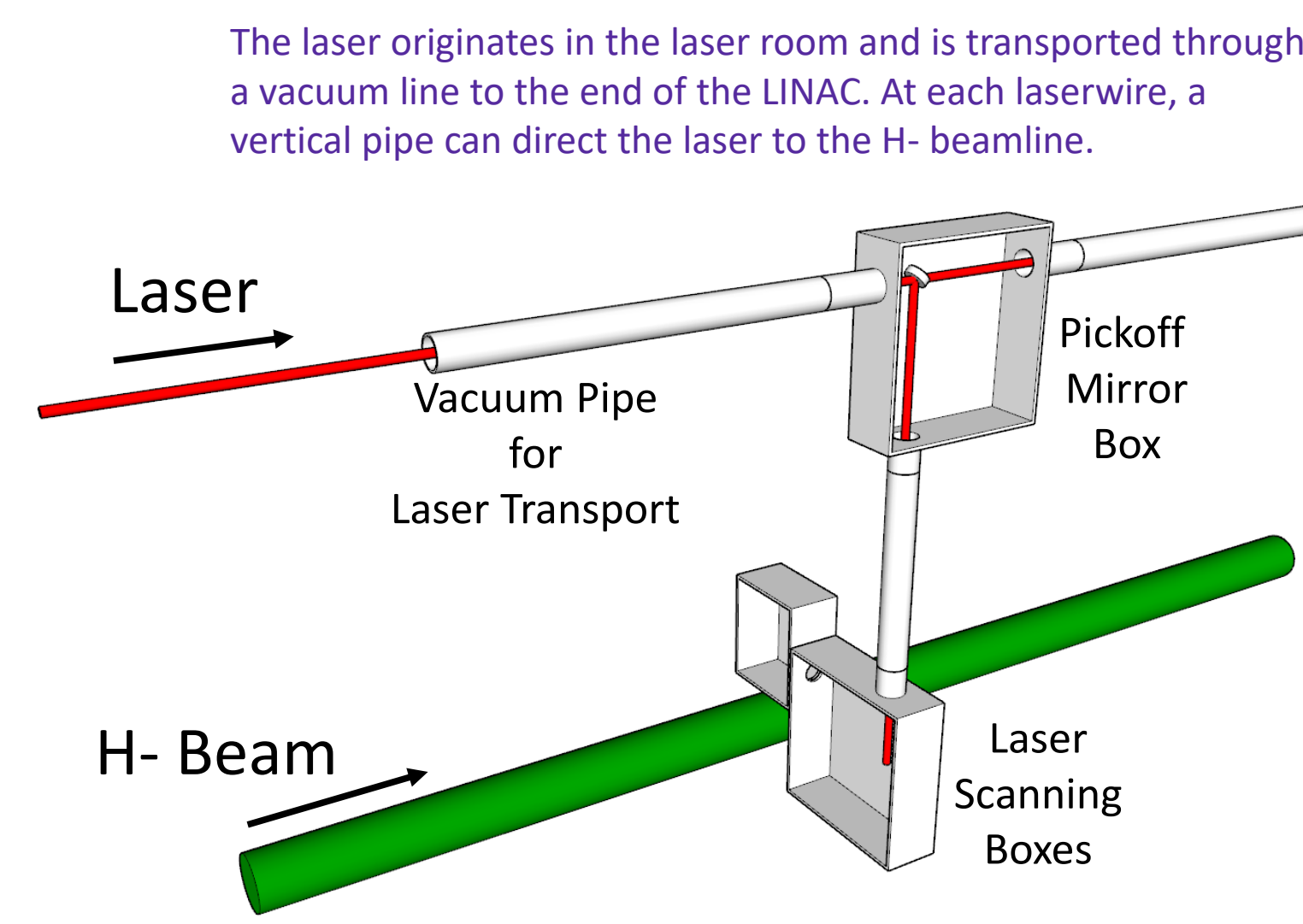
with \hat{l} and $\hat{\beta}$ being the laser and H⁻ normalized velocity vectors. See [4] for the origin of the square root multiplier. The cross section depends on the laser wavelength in the frame of the H⁻,

$$\tilde{\lambda}_l = \lambda_l \frac{\sqrt{1-\beta^2}}{1-\beta}$$

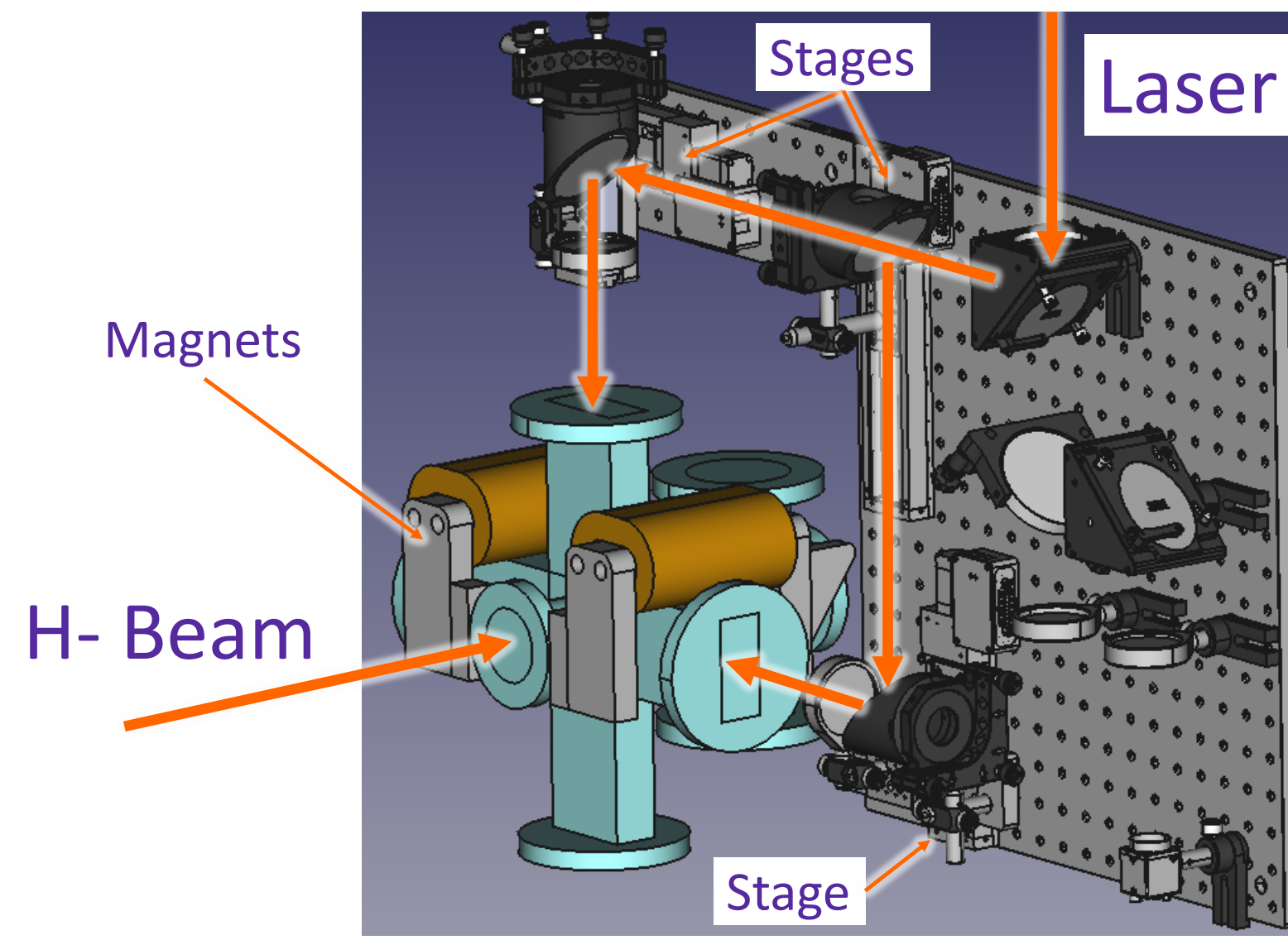
For orthogonal beams, the two equations reduce to

$$\tilde{\lambda}_l = \lambda_l \sqrt{1-\beta^2}$$

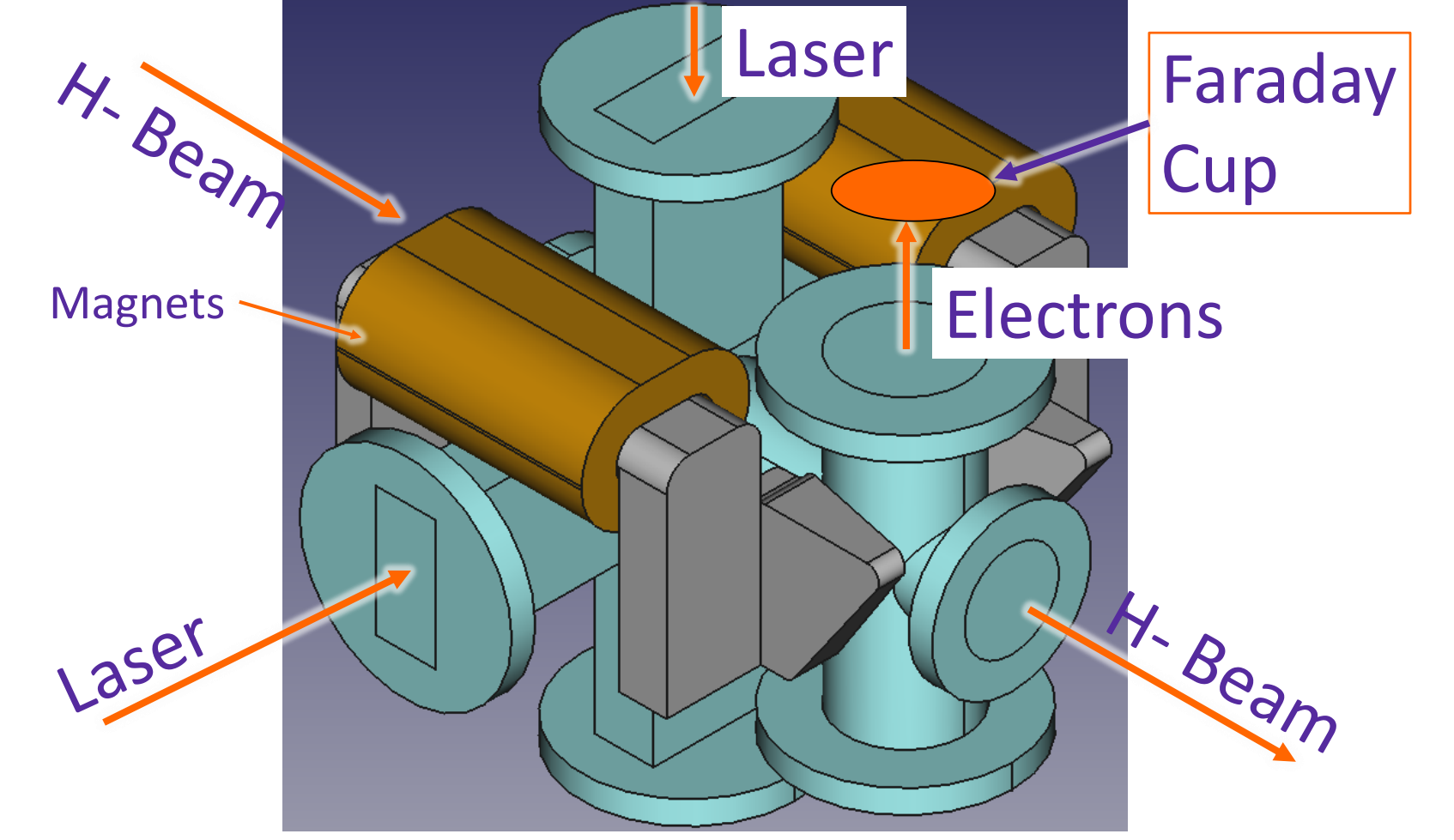
Experimental Device



Laser Scanning Box optics showing moving stages for scanning.



The incoming H⁻ beam is partially ionized by the laser and the electrons are bent vertically by a magnet to a Faraday cup. The blue volume is the vacuum chamber.



Laserwire positions and associated beam parameters

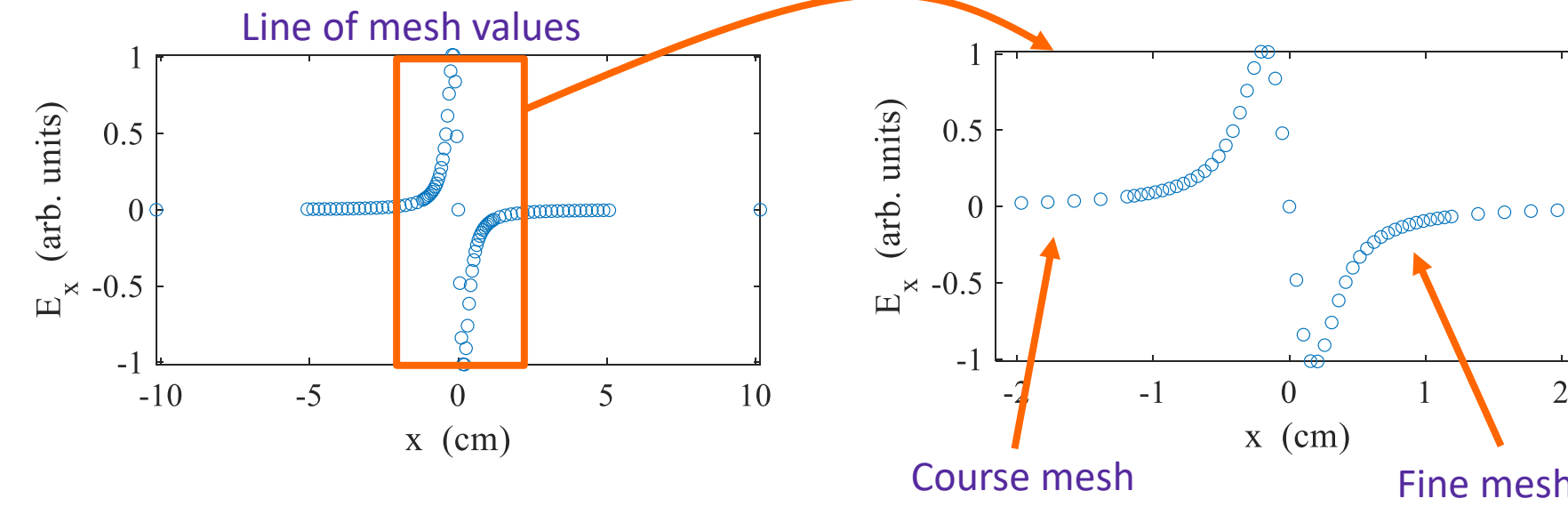
Laserwire Location	Position [m]	E _k [MeV]	σ _x [mm]	σ _y [mm]	σ _t [ps]
MEBT	18.7	2.1	2.3	2.3	208
HWR	25.4	10.0	1.3	1.4	33
SSR1 CM #1	31.6	18.6	1.2	1.2	20
SSR2 CM #1	51.5	61.2	1.4	1.5	13
SSR2 CM #4	65.2	106.0	1.3	1.3	13
SSR2 CM #6	78.9	153.9	1.4	1.4	11
LB650 CM #1	93.4	192.2	2.3	2.4	6.7
LB650 CM #3	107.1	267.4	1.8	1.9	5.7
LB650 CM #6	127.6	400.9	1.9	2.0	5.2
LB650 CM #9	148.0	516.5	2.1	1.8	5.0
HB650 CM #2	170.5	652.6	1.8	1.9	4.4
HB650 CM #4	192.9	833.3	1.5	1.9	3.7

Electromagnetic Field Calculations

The electromagnetic field calculations involve two separate parts: the fields of the H⁻ beam, and the static fields of both the electron collection magnets and possibly secondary electron containment electrodes.

Bunch Fields

The beam field calculation is done in MATLAB and uses a single bunch which can have any arbitrary shape and size, but a single fixed velocity. The fields are evaluated on a rectangular mesh containing an inner section with generally closer spacing to resolve the fields within the bunch, and an outer section with larger spacing. The fields at each mesh point are a numerical integration over the bunch charge. This numerical integration requires a mesh of the bunch as well. To reduce numerical errors, the field evaluation mesh spacing is adjusted such that it is an integer multiple of the bunch mesh spacing.



Laser Grid

Uses a fixed cylindrical mesh axially aligned with the laser and covering the overlap region of the laser and the H⁻ beam. The mesh is an elliptical cylinder with radii that scale with the transverse laser size. This keeps the mesh size proportional to the laser width and avoids losing resolution near the laser waist. Used when the laser intensity is low enough that depletion of the H⁻ is not important.

Tracking Simulation

The tracking simulation is written in MATLAB and was created originally to track electrons in the electron beam profiler [8] and ionization profile monitors [9]. It tracks the electrons through static fields and the fields of the H⁻ bunches but does not do self-interactions with the other electrons. It uses an adaptive Runge-Kutta method [10] to solve the pseudo-relativistic second-order differential equation of motion

$$\vec{F}(\vec{r}, t) = m \frac{d\vec{v}}{dt} = m \frac{d(y\vec{v})}{dt}$$

$$\vec{F}(\vec{r}, t) = m\gamma(\vec{a} + \gamma^2\vec{\beta}(\vec{\beta} \cdot \vec{a}))$$

which, when inverted to find \vec{a} , is

$$\vec{a} = \frac{d^2\vec{r}}{dt^2} = \frac{1}{\gamma m} (\mathbf{I} - \vec{\beta}\vec{\beta}^T) \vec{F}(\vec{r}, t)$$

where $\vec{F}(\vec{r}, t) = q(\vec{E}(\vec{r}, t) + \vec{v} \times \vec{B}(\vec{r}, t))$, m is the mass of the particle being tracked, $\gamma = 1/\sqrt{1-\beta^2}$ is the Lorentz factor, and \mathbf{I} is the identity matrix. We apply the Runge-Kutta method to the second-order differential equation rewritten as coupled first-order differential equations

$$\frac{d\vec{v}}{dt} = \frac{1}{\gamma m} (\mathbf{I} - \vec{\beta}\vec{\beta}^T) \vec{F}(\vec{r}, t)$$

$$\frac{d\vec{r}}{dt} = \vec{v}$$

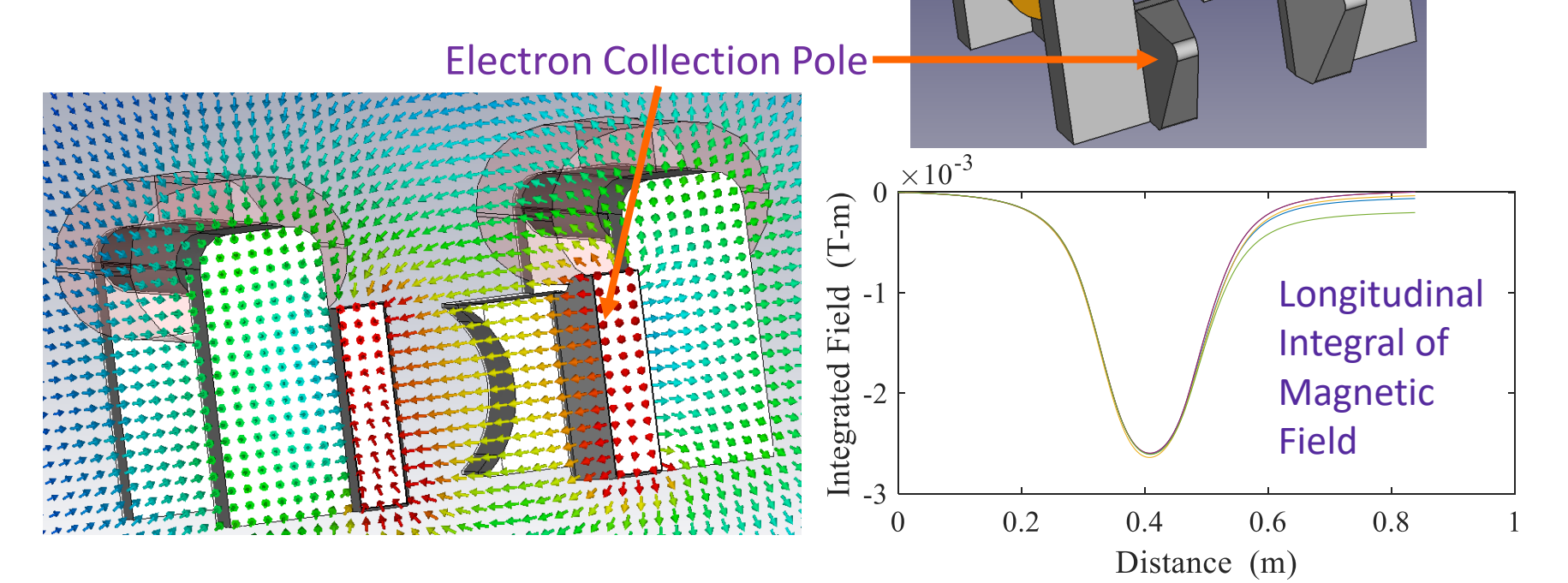
For the bunch fields, the field is interpolated to the requested position after adjusting it for the requested time and the velocity of the bunch,

$$\vec{E}[\vec{B}(\vec{r}, t) \rightarrow \vec{E}[\vec{r} + \vec{v}t_m]]$$

where $t_m = (t \text{ modulo } t_b)$. The modulo function implements a repetitive bunch structure at the specified bunch spacing, t_b . The adaptive part of the algorithm adjusts the step size to keep changes in the momenta, either absolute value or direction, within a range specified by thresholds. If any of the thresholds are exceeded, the step size is adjusted to compensate.

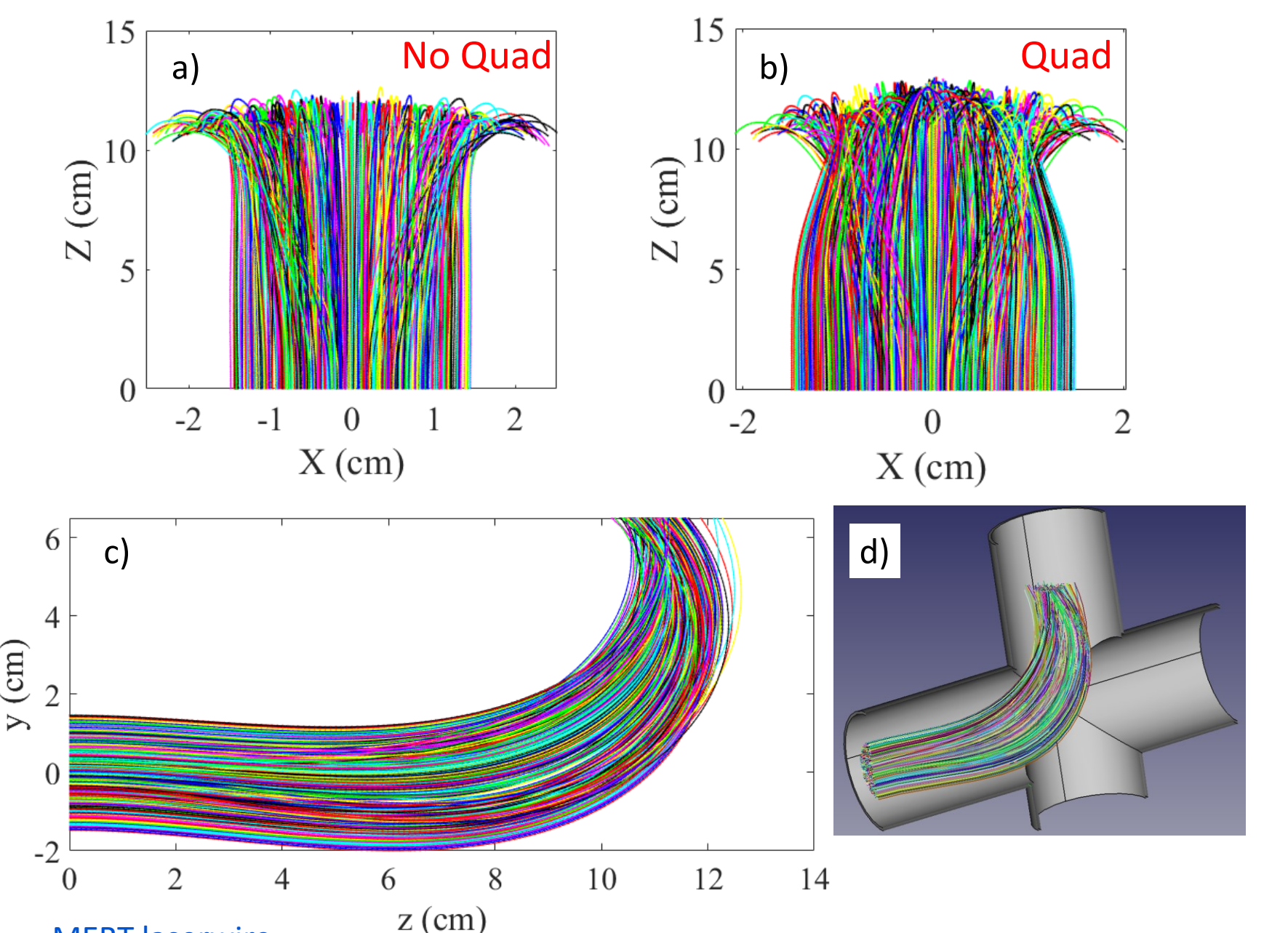
Static Fields

The static fields are calculated in CST [7] which is a 3D electromagnetic simulation. We designed a magnet with a return yoke to reduce the impact on the H⁻ beam. In addition, we will also add a small quadrupole magnet for the MEBT laserwire to compensate electron spreading from H⁻ space charge forces. When the electrons strike the Faraday cup, they generate secondary electrons that may escape the surface of the Faraday cup, altering the collected charge. To avoid this, we may need to install a conductive ring to apply an electrostatic field to keep the secondary electrons from leaving.



MEBT laserwire

a) and b) are the trajectories looking down from above the beam. They show the difference in final spread between having a quadrupole field and not having a quadrupole field.

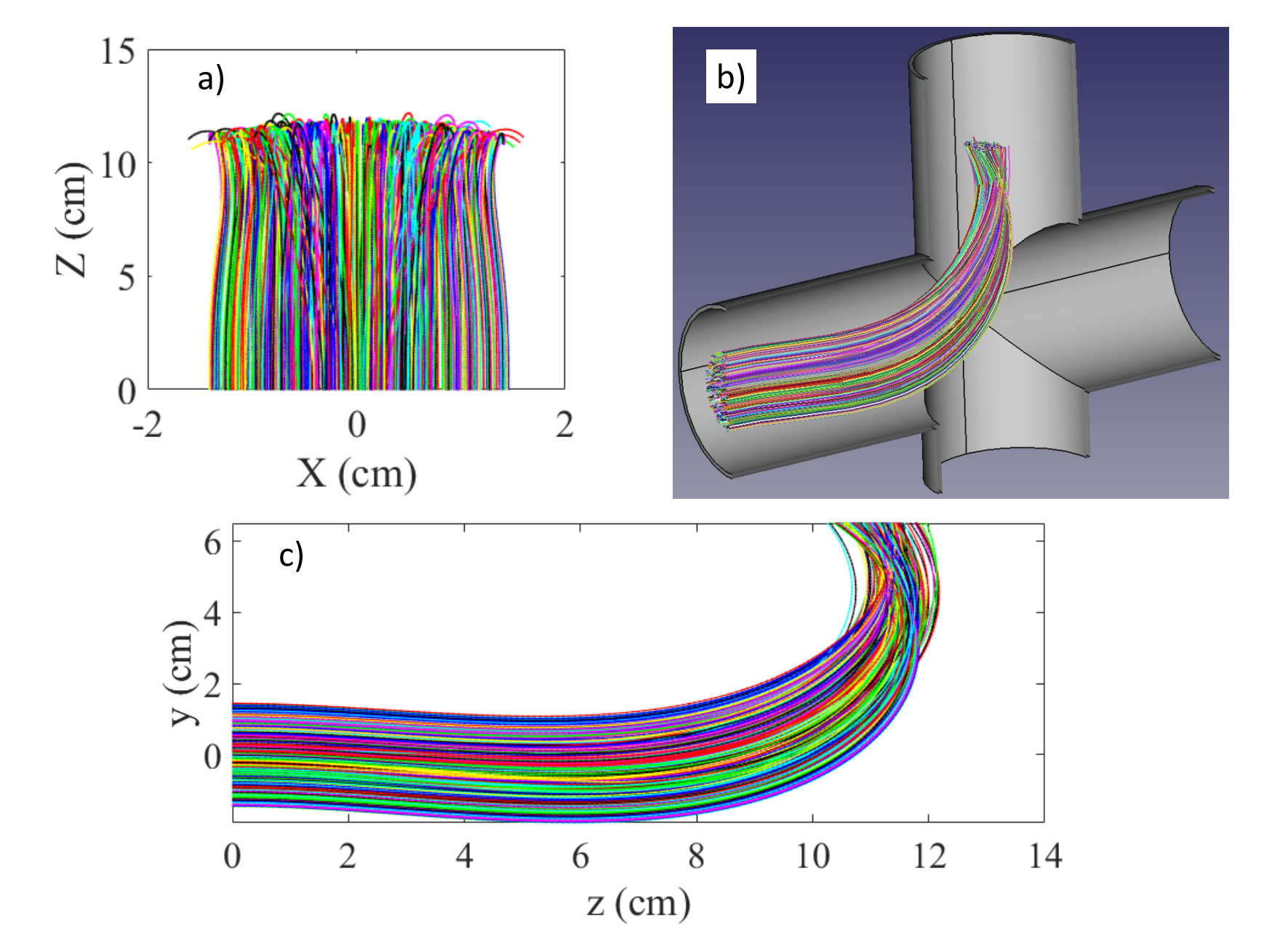


MEBT laserwire

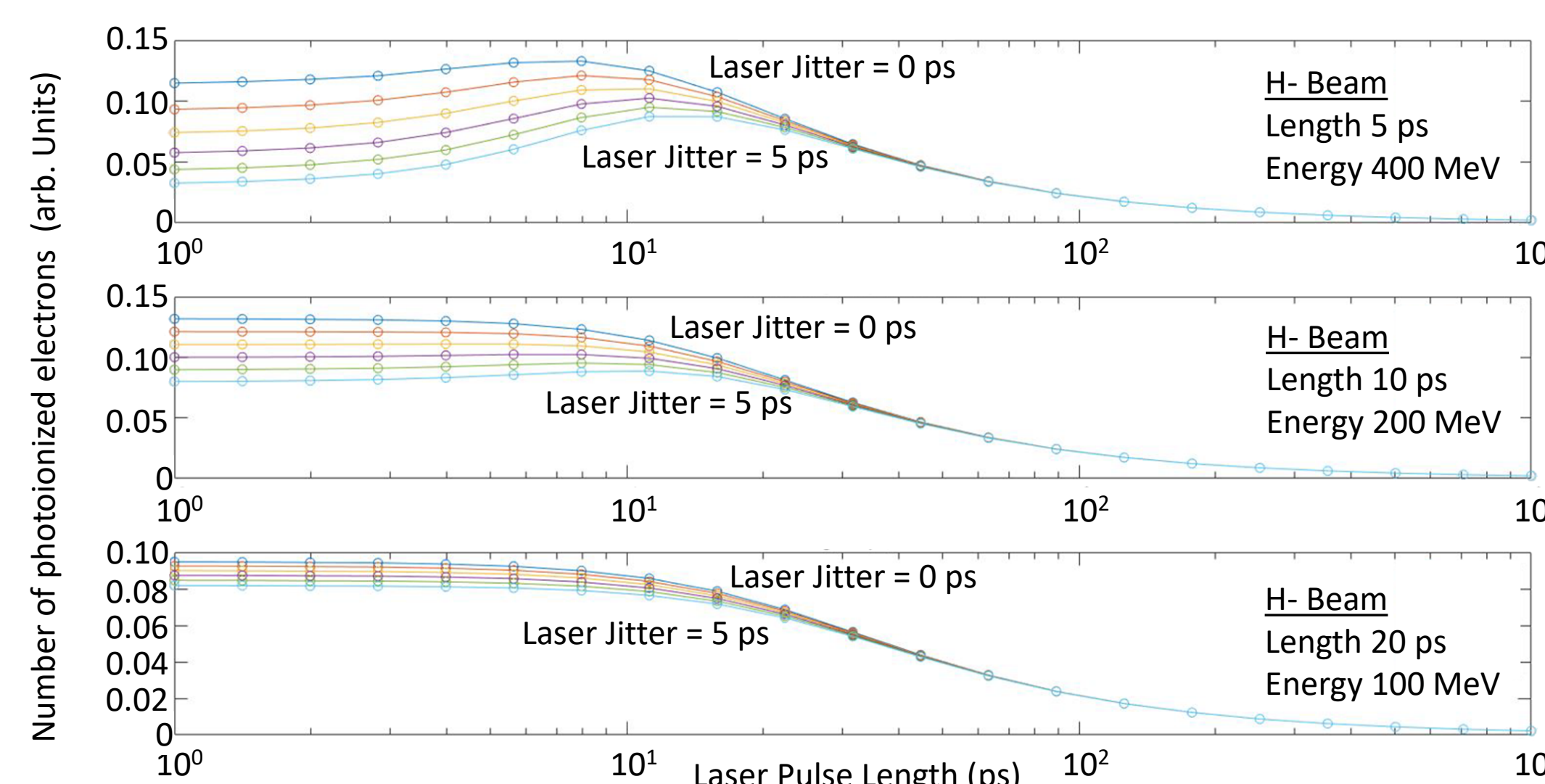
c) and d) are the trajectories looking from the side of the beam. They first deviate down before bending up which allows more clearance between the electrons and the beampipe.

HWR laserwire (after 1st cryomodule)

a) is the trajectories looking down from above the beam. Notice that the containment is much better even without the quadrupole since the energy is high enough to prevent significant spreading from H⁻ space charge. b) and c) are the trajectories looking from the side of the beam.

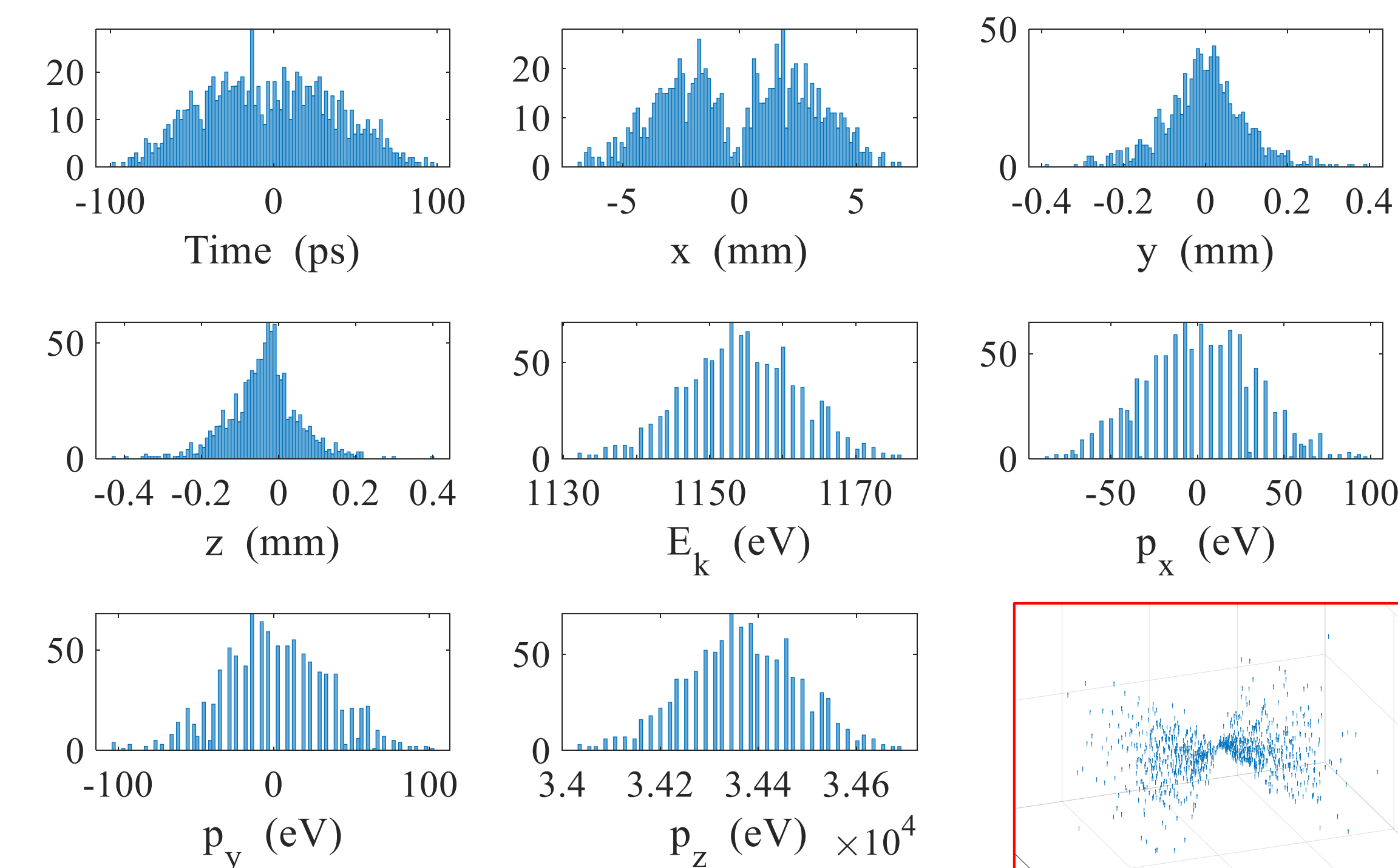


Studies were done to evaluate the photoionization rates for different length laser pulses, laser arrival time jitter, and H⁻ temporal bunch lengths. These results will help to determine the optimal laser properties to maximize signal and resolution while minimizing unused laser energy which has detrimental effects on the vacuum windows. For instance, from the plots, we can see that laser pulses with a length of 20 or 30 ps have good photoionization but small variation with jitter.



Electron Generation

Electrons for tracking are generated from the space-time mesh containing the calculated number of photoionizations. A Poisson distribution is utilized for up to 500 electrons, beyond which a Gaussian approximation is used. The electrons are given momenta based on the 6D phase space specified for the H⁻ beam.



3D distribution of electrons. The laser waist is evident here.

REFERENCES

- [1] V. Lebedev et al., "The PIP-II conceptual design report", FNAL, Batavia, IL, USA, Rep. FERMILAB-DESIGN-2017-01, Mar 2017. doi:10.2172/1346823
- [2] Y. Liu et al., "Laser based diagnostics for measuring H⁻ beam parameters", in Proc. PAC'11, New York, NY, USA, Mar-Apr. 2011, pp. 1433-1437. https://accelconf.web.cern.ch/PAC2011/papers/weocn1.pdf
- [3] V. Scarpine et al., "Beam profile measurements utilizing an amplitude modulated pulsed fiber laser at PIP-II", in Proc. IBIC'21, Korea, Sept 2021. doi:10.18429/JACoW-IBIC2021-TUPP25
- [4] L.D. Landau and E.M. Lifshitz, The Classical Theory of Fields. Oxford, England: Pergamon Press, 1975, pp. 34-36.
- [5] J.T. Broad and W.P. Reinhardt, "One- and two-electron photoionization from H⁻: A multichannel J-matrix calculation", Phys. Rev. A, vol. 14, p. 2159, 1976. doi:10.1103/PhysRevA.14.2159
- [6] MathWorks. https://www.mathworks.com
- [7] Dassault Systemes - Simulia. https://www.3ds.com
- [8] R. Thurman-Keup et al., "Commissioning and First Results of the Electron Beam Profiler in the Main Injector at Fermilab", in Proc. IBIC'17, Grand Rapids, MI, USA, Aug. 2017, pp. 330-334. doi:10.18429/JACoW-IBIC2017-WEA3B3
- [9] J.R. Zagel et al., "Third Generation Residual Gas Ionization Profile Monitors at Fermilab", in Proc. IBIC'14, Monterey, CA, USA, Sep. 2014, pp. 408-411. https://jacow.org/IBIC2014/papers/tupd04.pdf
- [10] https://en.wikipedia.org/wiki/Runge%E2%80%99s_Kutta_methods
- [11] Y. Liu et al., "Longitudinal bunch profile measurement of operational H⁻ beam using laser wire and virtual slit", Phys. Rev. Accel. Beams, vol. 26, p. 042801, 2023. doi:10.1103/PhysRevAccelBeams.26.042801